Bacterial quorum sensing allows graded and bimodal cellular responses to variations in population density

Jennifer B. Rattray[1,2], Stephen A. Thomas[1,2,3], Yifei Wang[1,2,4], Evgeniya Molotkova[1], James Gurney[1,2], John J. Varga[1,2], Sam P. Brown[1,2]

[1] School of Biological Sciences, Georgia Institute of Technology, Atlanta, 30332 GA, USA
[2] Center for Microbial Dynamics and Infection, Georgia Institute of Technology, Atlanta, 30332 GA, USA
[3] Graduate Program in Quantitative Biosciences (QBioS), Georgia Institute of Technology, Atlanta, 30332 GA, USA
[4] The Institute for Data Engineering and Science (IDEaS), Georgia Institute of Technology, Atlanta, 30332 GA, USA

Corresponding author: Sam P. Brown

Email: sam.brown@biology.gatech.edu

ORCIDs. Jennifer B. Rattray https://orcid.org/0000-0003-3478-2242; Stephen A. Thomas http://orcid.org/0000-0003-0773-0236; Yifei Wang http://orcid.org/0000-0002-7510-7959, James Gurney http://orcid.org/0000-0002-8364-3380, John J. Varga https://orcid.org/0000-0002-4868-1971

Keywords

Bacterial communication, quorum sensing, sociomicrobiology, reaction norm

Author Contributions

J.B.R and S.P.B. conceived the idea and designed the experiment; J.B.R., E.M., J.G., and J.J.V. performed the experiments; J.B.R analyzed the data; and J.B.R., S.A.T, Y.W., J.G., J.J.V., and S.P.B. wrote the paper.

Abstract

Quorum sensing (QS) is a mechanism of cell–cell communication that connects gene expression to environmental conditions (e.g. density) in many bacterial species, mediated by diffusible signal molecules. Current functional studies focus on a dichotomy of QS on/off (or, quorate / sub-quorate) states, overlooking the potential for intermediate, graded responses to shifts in the environment. Here, we track QS regulated protease (*lasB*) expression and show that *Pseudomonas aeruginosa* can deliver a graded behavioral response to fine-scale variation in population density, on both the population and single-cell scales. On the population scale, we see a graded response to variation in environmental population density. On the single-cell scale, we see significant bimodality at higher densities, with separate OFF and ON sub-populations that respond differentially to changes in density; static OFF cells and increasing intensity of expression among ON cells. While the QS-controlled behavioral output is graded, the underlying multi-signal dynamics display a threshold shift in signal concentration with increasing density, reflecting the onset of positive signal auto-regulation at intermediate densities. Together these results indicate that QS can tune gene expression to graded environmental change, with no critical cell mass or 'quorum' at which behavioral responses are activated on either the individual cell or population scale. In an infection context, our results indicate there is not a hard threshold separating sub-quorate 'stealth' mode and a quorate 'attack' mode.

Main Text

Introduction

Many species of bacteria are capable of a form of cell-cell communication via diffusible signal molecules, generally referred to as quorum sensing (QS). The study of QS has largely focused on the intracellular gene regulatory scale, leading to a detailed understanding of the regulatory mechanisms shaping the production of and response to signal molecules in model organisms such as *Vibrio cholerae*, *Bacillus cereus* and *Pseudomonas aeruginosa* (1–3). We now understand that QS is mediated by multiple diffusible signals that together control a diverse array of responses, including swarming, luminescence, competence and the production of diverse secreted factors (4, 5)

While the molecular mechanisms of QS have been described for model organisms in remarkable detail, the functional and evolutionary context of QS continues to be disputed. In other words, while we now have a better understanding of *how* QS works, we still have limited understanding of *why* bacteria use this system to control behavior. What are the functions of QS? How do these QS functions help bacteria to survive and grow? The standard answer is that bacteria use QS to

sense when they are at sufficient density ('quorate') to efficiently turn on cooperative behaviors such as secretion of toxins and enzymes in order to collectively modify their environment (6). Other researchers have argued that QS is an asocial sensing apparatus, where individual cells produce and monitor signal levels in order to infer their physical environment (am I in an open or enclosed space?) (7). More recently, integration of molecular and evolutionary approaches has increased the menu of potential functions to include sensing multiple aspects of both the social and physical environment (6, 8–10) and coordinating complex social strategies that limit the profitability of non-cooperating 'cheat' strains (11–18).

A critical step in assessing the various adaptive hypotheses is establishing the functional capacities and limits of QS. Previous studies have demonstrated 'density sensing' functions – populations can use QS to sense when they exceed a density threshold (6, 19, 20). In addition, Darch et al. (2012) demonstrated that responding with increased QS controlled cooperative activity at high density can provide a fitness benefit (6). Other studies have demonstrated 'diffusion sensing' functions (7) – QS systems can functionally respond to variation in physical containment, so that even a single cell can become 'quorate' (turn on a QS controlled reporter gene) if isolated in a sufficiently small contained space (9). More recently, some studies have demonstrated 'genotype sensing' functions – QS can respond to variation in the genotypic composition of a population, restricting QS-controlled responses to populations that are enriched with wildtypes (11, 14, 21, 22).

The functional studies outlined above largely focus on a dichotomy of QS on/off (or, quorate / sub-quorate) states, overlooking the potential for intermediate, graded responses (Fig 1A). The threshold quorate/non-quorate concept is ingrained in the QS literature following the use of the legal 'quorum' analogy (20), and is also supported by mathematical models of QS signal dynamics that highlight how sufficiently strong positive feedback control of signal production can produce a sharp threshold response to changes in environmental parameters such as density or diffusion (23, 24). However, these same mathematical models indicate that graded responses are also possible, dependent on the model parameterization. More generally, Fig 1A highlights that the phenotypic response of QS bacteria to differing environmental conditions can be viewed as a 'reaction norm' (25–28) that can in principle take differing shapes. Reaction norms describe phenotypic responses of a single genotype (y-axis, Fig 1A) to varying environmental inputs (x-axis, Fig 1A). Incorporating a reaction norm framework provides a menu of quantitative metrics to define QS responses to environmental variation (e.g., slope, intercept, and variances). With this reaction norm framework, it is important to emphasize that in our study the x-axis is not time, but instead captures a gradient of environmental conditions. Whether responses are graded or thresholded during the growth towards high density is a separate line of inquiry (29). Describing

the reaction-norms of QS cells and populations to contrasting environments is an important step towards understanding the capacities of QS systems to differentially respond to novel environments.

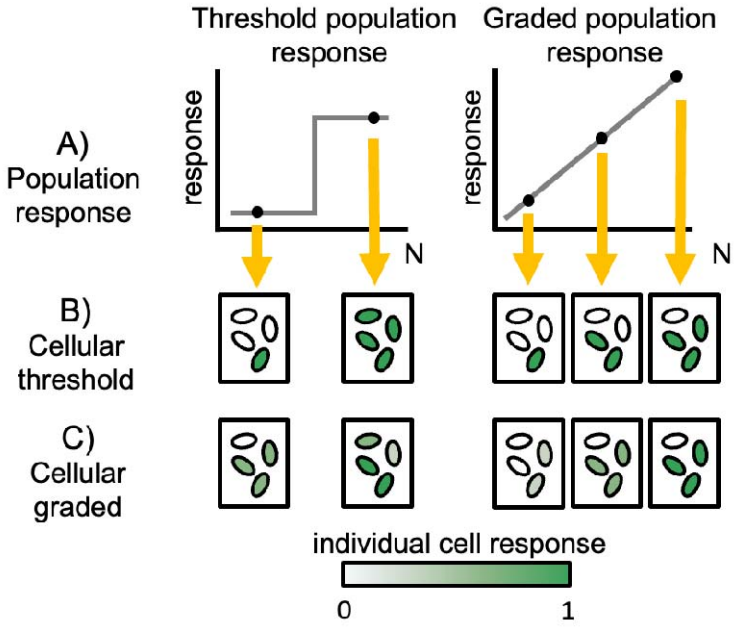

Figure 1. Schematic of potential population and single cell responses to variation in cell density. A) Population response (y-axis) across discrete carrying capacity environments (N, x-axis), given a threshold (left) or graded response (right). In (B) and (C) we outline alternative cell-scale responses (intensity of green cells) that are consistent with discrete population scale behaviors (yellow arrows). (B) threshold (ON/OFF) cellular responses can produce a threshold or graded responses on population scale. (C) graded individual responses can produce threshold or graded responses on a population scale.

Whether the population scale reaction norm to environmental variation is threshold-like or graded (Fig 1A), a separate question is how collective population-level responses are constructed out of individual cellular contributions (Fig 1B,C). Studies of QS on a single-cell scale have revealed substantial heterogeneity in response to QS signals (9, 30–36), highlighting that cell-cell communication does not necessarily result in tight synchronization of individual cell activity (Fig 1B,C). In some systems, heterogeneity can be quenched by the addition of extra signal (31, 33), implying a lack of receptor saturation. However, this is not a universal result (30), indicating that other molecular processes can drive cellular variation in response. Regardless of the molecular details, we currently lack a behavioral understanding of how individual cellular responses vary with changes in the environment.

In the current study we address the canonical 'density sensing' function of QS, using the environmental generalist and opportunistic pathogen *Pseudomonas aeruginosa*, and an

unprecedented scale of environmental resolution (13 discrete limiting carbon levels conducted in triplicate, generating 39 density environments). Our first challenge is to map the population scale resolving power of QS to quantitatively discriminate graded differences in population density (Fig 1A). Does *P. aeruginosa* respond in a purely threshold manner, collapsing quantitative differences in population density into a simple low / high qualitative output, or can QS allow *P. aeruginosa* to deliver a graded response to distinct environmental densities? Our second challenge is to understand how collective responses are partitioned across individual cells. Are changes in collective responses governed primarily by changes in the proportion of cells in an on state (Fig 1B) or changes in the individual cell intensity of response (Fig 1C), or both?

Results

Collective level of response to density is graded and linear. Our first challenge is to map out the population scale reaction norm of the collective QS-controlled protease (*lasB*) response to variation in population densities. To provide a detailed picture of the QS response reaction norm to varying density, we grew a QS reporter strain (PAO1 pMHLAS containing the *PlasB::gfp(ASV)* reporter construct for QS regulated protease expression (37)) under 13 conditions of carbon limitation in triplicate and measured average fluorescence output per cell as the populations reach carrying capacity (Fig 2). Dead cells with compromised membranes were identified with a propidium iodide stain and excluded from analysis. The range of cell densities generated from this method is from $1x10^8$ cells/ml to $2x10^9$ cells/ml. Figure 2 shows that QS response is linear with increasing culture density, providing intermediate levels of average per-capita response to intermediate densities. To confirm the lack of threshold behavior we assessed alternate statistical models including threshold functions, and found that a linear fit model supports the data better than a step-function fit (AIC linear: 89, AIC step-function: 190; relative likelihood that the linear model is the best fit compared to step-function > 10^9, see (38)), supporting a graded population response as outlined in Figure 1. This agrees with literature that QS induction at lower population densities is possible (6, 9, 19), but differs in that there is no observable population density at which populations ‘switch’, or reach quorum, into a responsive state.

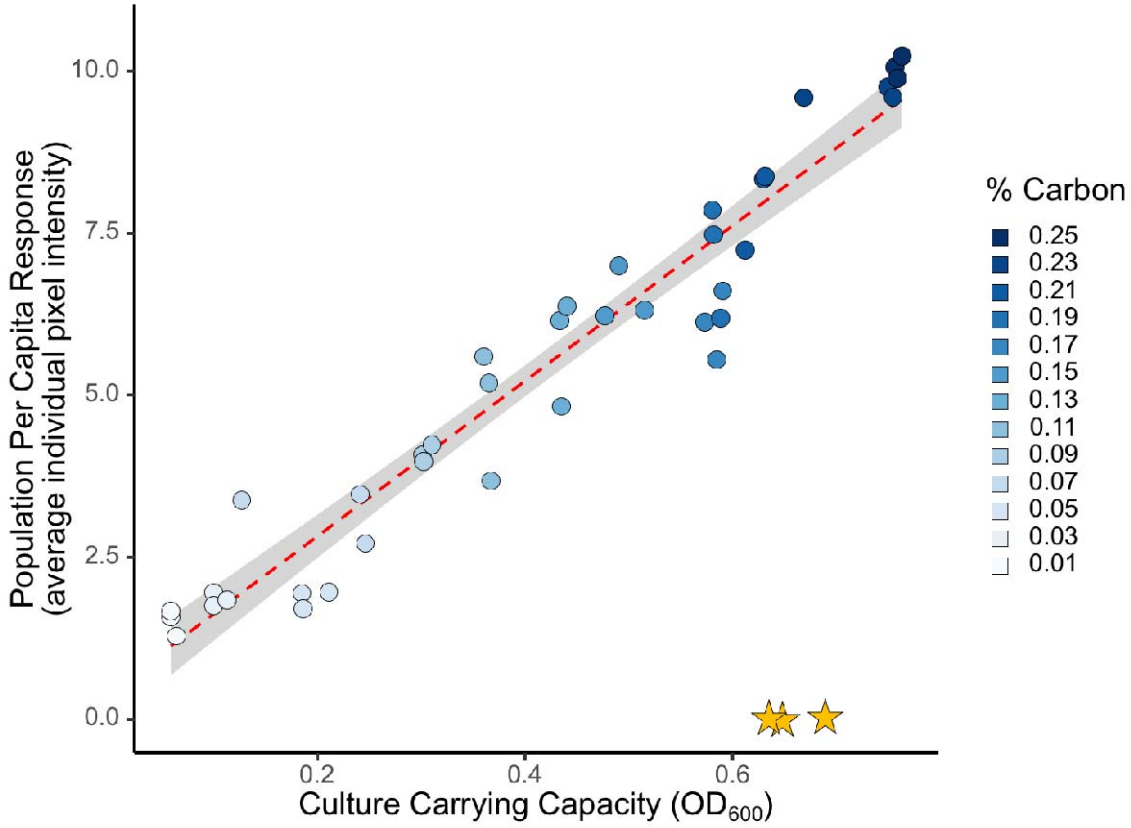

Figure 2. Population response to increasing cell density is linear and graded. 13 distinct culture carrying capacities were generated by manipulating the concentration of casein as the limiting resource (Fig S1). Cells were grown to carrying capacity in triplicate and immediately assayed for QS response via fluorescence microscopy imaging. Response is determined by a fusion of the quorum sensing controlled *lasB* promoter and an unstable green fluorescent protein (PAO1 pMHLAS containing *PlasB::gfp(ASV)*). Individual cell pixel intensity is a measure of cellular quorum sensing response and average pixel intensity is calculated across all cells in the population as a proxy for total population expression. Microscopy averages are congruent with population scale plate reader results (Figure S2). A quorum sensing signal knockout (Δ*lasI*Δ*rhlI*), yellow star, shows background response with no signal in the environment. Average population investment in QS increases as culture density increases with no observable density threshold (AIC linear: 89, AIC step-function: 190).

Individual response to density is bimodal at high densities. Figure 2 establishes that on a collective population scale, the response to environmental variation (in density) is smoothly graded. Next, we ask how this collective response is built from individual cell contributions. Is the graded increase due to more cells turning on at higher densities (Figure 1B), cells turning on to a greater extent (Figure 1C), or both? To address this question, we take the same data presented

in Figure 2 and now present the distribution of individual cellular responses rather than simply the mean response (Figure 3).

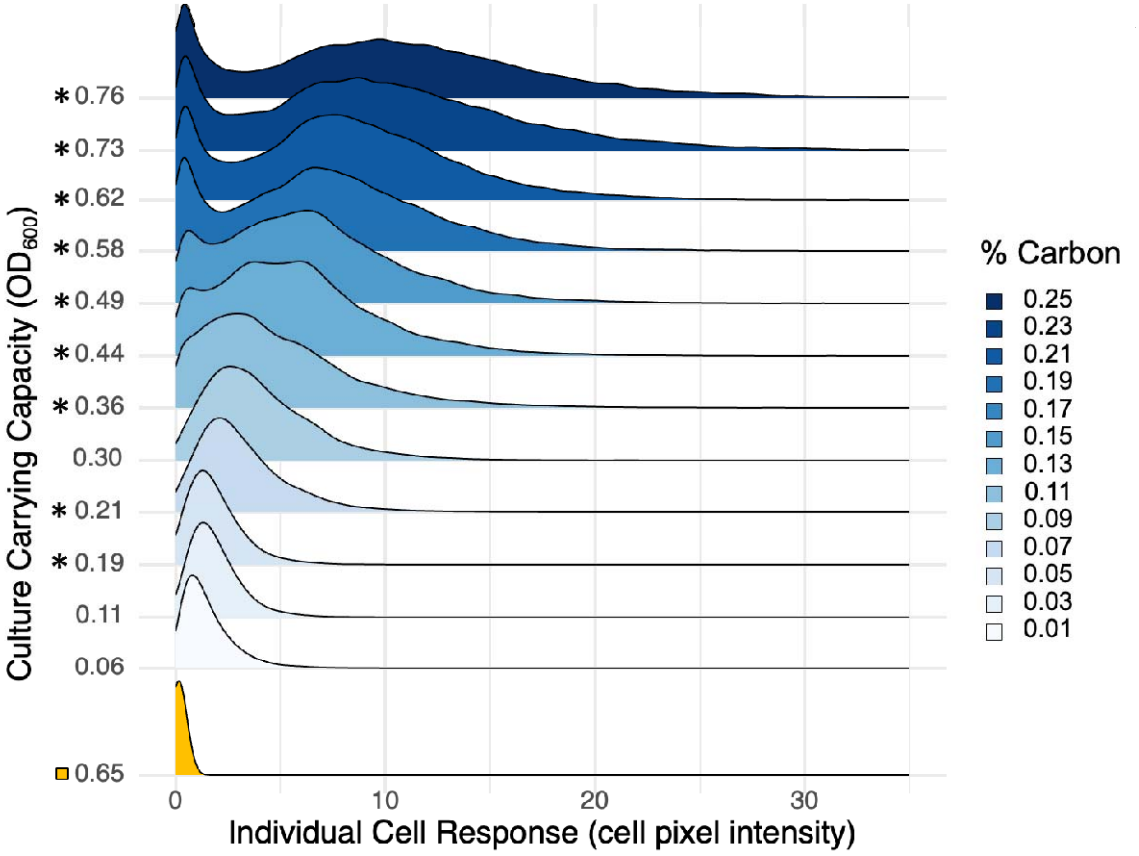

Figure 3. Individual response is heterogenous and bimodal at higher densities. Ridgeline density plot (bandwidth = 0.435) of single-cell *lasB* reporter response data showing the distribution of individual cell QS expression across the population. For brevity and plotting purposes, carrying capacities were averaged across 3 replicates for each of the 13 carbon environments before plotting. A full plot of each independent replicate environment can be found in Figure S3. Each line summarizes 18,000 to 30,000 individual cell measurements, scaled to a unit height. Asterisks indicate significant bimodality (Hartingan's Dip Test (39), Figure S4). The quorum sensing signal knockout (*ΔlasIΔrhlI*) is denoted with yellow boxes. A total of 345,000 individual cell measurements were analyzed.

As expected from prior studies in other QS systems (9, 30–36), plotting all individual responses within a population shows cell-to-cell variation in QS response within a single population despite isogenic and homogenous culture conditions (Figure 3). In addition, at higher densities we see significant bimodality (defined by Hartigan's Dip Test, Figure S4), with the population segregating into an unresponsive, sub-quorate, OFF state and a responsive, quorate, ON state.

In light of this bimodality, we fit a two-component finite mixture model to the data (Figure 4A, see Figures S10-S13 and Table S2 for extended analysis), which allows us to define the average intensity of the ON state (Figure 4B) and the proportion of cells in the OFF or ON states (Figure 4C).

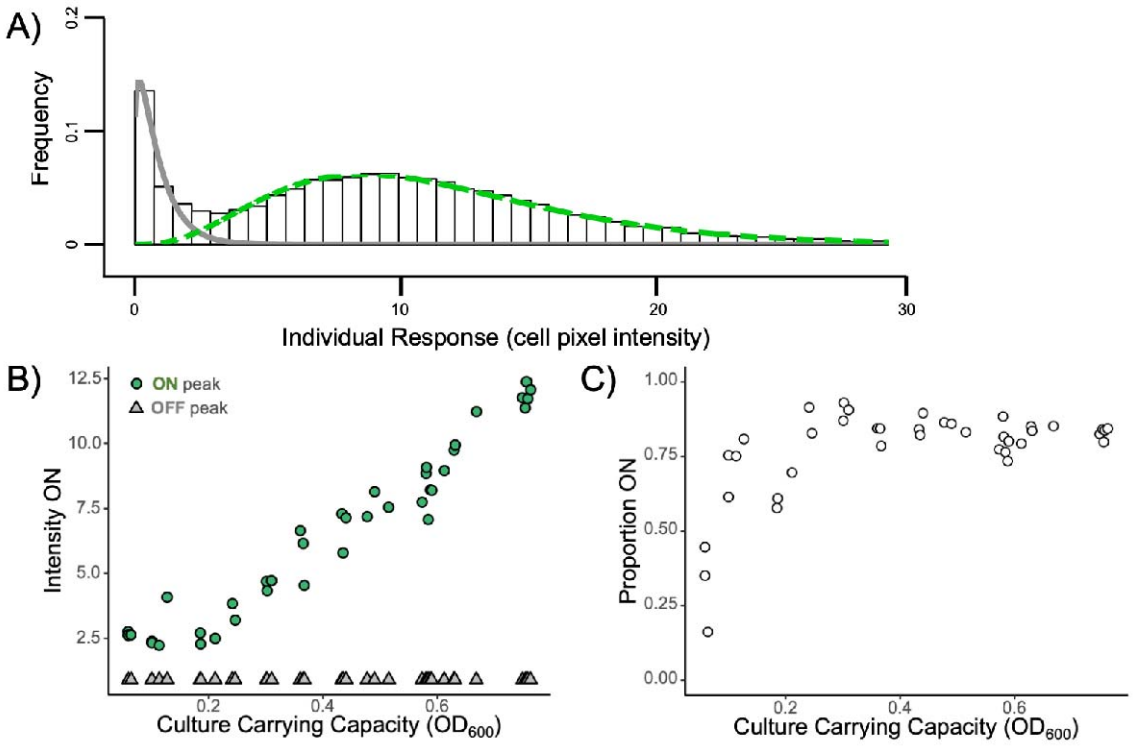

Figure 4. Proportion of cells responding and level of response varies with density. In light of the bimodal responses in Figure 3, we course-grain the single-cell *lasB* response data into discrete ON/OFF states. A) Method summary. We quantify distinct ON/OFF states by fitting a two-component finite mixture model at each measured optical density, where the OFF state is fixed to the OFF state of the highest density environment. The histogram shows the distribution of cellular expression levels at a single density treatment (0.76 OD_{600}), the grey line is the fitted OFF state and the green dashed line is the fitted ON state. B) The mean intensity of the ON (green circle) and OFF (grey triangle) states is determined from the means of mixture model component fits (green and grey lines in panel A). The mean intensity of the ON state distribution increases as culture density increases, while the mean of the OFF state remains constant. C) The proportion of cells ON in the population is determined from the relative mass of cells in the model component fits. The proportion ON increases with culture density but does not reach 100%.

Figure 4B illustrates a graded linear increase in the intensity of the ON state with increasing environmental density, and a density-invariant off state. Figure 4C illustrates that the proportion of cells that are ON plateaus at around 85% at densities with consistent support for bimodality (above 0.36 OD_{600}). At lower densities, the intensity of the ON state (Figure 4B) declines to a point where the OFF and ON states are no longer significantly different and the dip test fails to reject uni-modality (Figure S4). In supplemental materials, we present alternate statistical

185 analyses of this data, and of other related datasets. Across other experiments, we find consistent
186 support for the graded and bimodal response pattern on the single-cell scale across multiple
187 assay time-points (Figure S5) and across two reporter strain constructs (Figure S6) and support
188 for the graded and linear response pattern on the population scale across fluorescent and lux
189 reporters (Figure S2, Figure S7). We find further support for the graded reaction norm on the
190 population scale across two additional QS controlled genes (*pqsA, rhlI;* Figure S7).
191
192 As quorum sensing is a signal mediated behavior, we sought to connect these behavioral results
193 with the underlying signaling dynamics in the environment. QS in *Pseudomonas aeruginosa* is
194 heavily studied in a high-density context, revealing a complex mechanism of multi-signal control
195 (40–42). The *P. aeruginosa* QS system is dominated by the acyl-homoserone lactone (AHL)
196 signaling systems LasI/R and RhlI/R (40, 43). Each of these signaling systems codes for a signal
197 synthase (LasI, RhlI), which guide the production of a diffusible AHL signal molecule (3-oxo-C12
198 HSL, C4-HSL) at an initially basal level. Binding of each signal to its cognate receptor (LasR,
199 RhlR) results in an active transcriptional factor which can up-regulate cognate synthase activity
200 (signal auto-induction) along with other genes in the QS regulon. For more details on the
201 complexities of *P. aeruginosa* QS wiring, see (44–47).
202
203 In light of this established mechanistic understanding of high-density behavior, we outline three
204 alternate hypotheses for the reaction norms of multi-signal concentrations on density: (1) First,
205 under a null model of no autoinduction, we predict a linear increase in signal concentration,
206 reflecting a constant (baseline) per-capita signal production. (2) Second, under a threshold model
207 for the onset of autoinduction we predict a piecewise linear reaction norm, with a steeper slope in
208 the higher density environment (reflecting higher per-capita signal production following a
209 threshold onset of auto-induction). (3) Third, under a graded onset model, we predict a smoothly
210 accelerating reaction norm, with the slope at a given density reflecting the graded degree of onset
211 of autoinduction.
212
213 To test these hypotheses, we measured the environmental concentration of 3-oxo-C12 HSL and
214 C4-HSL from previous experiments (at the time point of QS response assays, Figure 3) using *E.*
215 *coli* biosensors (48) (Figure 5). To discriminate among the three explicit models, we fit multiple
216 alternate models to the data and compared their goodness of fit using information criteria. (Figure
217 5; Tables S3-S5 and Figures S14-S15). A linear fit, representing no positive signal auto-
218 regulation, is the worst of the models considered for both 3-oxo-C12 HSL and C4 HSL data.
219 Further statistical tests provide additional evidence for a non-linear relationship (Table S5). In
220 Figure 5, we show model fits for the best fitting continuously accelerating functions alongside a
221 threshold model fit. Evaluating these two models via AICc values (corrected AIC to account for

smaller datasets (38)) we find that the threshold model is the best supported model for both the 3-oxo-C12 HSL and C4 HSL data (Figure 5, inset). More specifically, we can assess the strength of support for the threshold model via the relative likelihood versus the next-best exponential model (38). For the C4 HSL data, we find the threshold model has 14-fold greater support, and for the 3-oxo-C12 HSL data, the threshold model has 8-fold greater support (Table S5). This analysis indicates there is a critical intermediate density that triggers an abrupt shift in the extent of signal auto-regulation, separating a basal signal regime from a higher density auto-regulated regime.

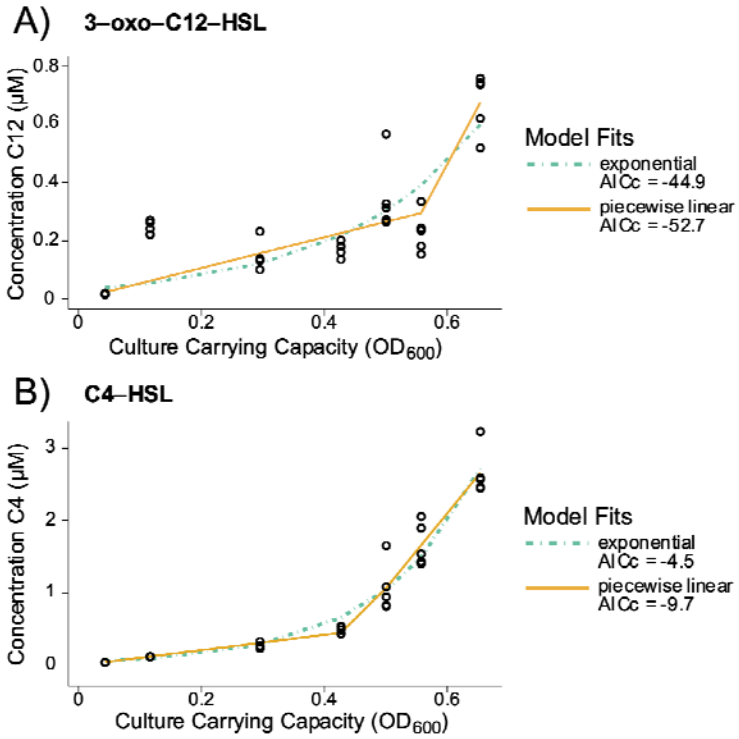

Figure 5. 3-oxo-C12 HSL and C4 HSL concentration increases in a threshold (piecewise linear) manner with increasing density. Signal environment was characterized using filtered culture supernatant (extracted at the same timepoints as for the gene expression data in Figure 3) and *E. coli* biosensors (48). Model fits are based on nonlinear least squares estimates. Model performance was assessed via AICc (see figure insets and Table S5). See Tables S3-S5 and Figures S14-S15 for statistical analysis details.

Discussion

Our results show that populations of *P. aeruginosa* can respond in a smoothly graded manner to variation in environmental density (Figure 2), and that populations exhibit significant bimodality at higher densities (Figure 3), and that this population scale graded response can be described by the number of responsive 'ON' cells and the intensity of the 'ON' state (Figure 4). Turning to the underlying signal mechanics, we further illustrate a threshold onset of signal auto-induction at

intermediate densities (Figure 5). The ability to achieve a graded population scale response implies in principle that *P. aeruginosa* can tune collective responses (such as the secreted elastase virulence factor produced by our *lasB* reporter gene) to graded environmental changes, rather than simply course-graining into a simple 'high / low' dichotomy. A similar population scale graded response to continuous environmental variation is visible in the data from Allen et al., which looked at variation in the genotypic composition of mixed populations grown to the same total density (11). As the proportion of wildtype (PAO1 versus Δ*lasR* 'cheats') increased, the wildtype per-capita investment in cooperative LasB secretions also increased, providing a simple behavioral mechanism to protect cooperative investments from exploitation by cheats (11, 22).

The existence of graded population scale responses across two continuously varying environmental inputs (density, genotypic composition) raises the question of why use a graded response? Is there an evolutionary rationale for a graded response, or is a graded increase simply the 'best approximation' of a threshold response, given a simple system working under genetic constraints? Existing evolutionary theory suggest that graded investment reaction norms can be adaptive, under a range of distinct scenarios (49, 50) (34, 35). In the specific context of quorum-sensing bacteria, evolutionary theory suggests that population scale responses to increasing density should depend critically on the shape of the cost and benefit functions of increasing cooperative investments. Specifically, a graded response is predicted to be the optimal strategy if the benefit function is decelerating and costs are linear with increasing investment (51).

To further consider the functional context of the graded reaction norms, we turn to the single cell scale data, which reveals how the graded population response is built from the contributions of individual cells. In agreement with previous work in multiple quorum-sensing organisms (9, 30–36, 52, 53), we find cell-scale heterogeneity. In addition, our results illustrate how cellular heterogeneity changes with the environment, demonstrating the onset of ON/OFF bimodality at intermediate densities, with both the proportion of cells ON and the intensity of the cellular ON states increasing with increases in culture carrying capacity (Figures 3 & 4).

The presence of a bimodal QS response is in contrast with the common view of QS as a mechanism of cell synchronization yet can be viewed as a striking example of widely observed cellular heterogeneity under QS control. Indeed, bimodal responses are implicit in some of the previous single-cell QS literature (31, 32, 53), for example Darch et al. (2018) report distinct populations of QS-responsive and non-responsive cells within single experimental runs (53). The degree of heterogeneity in any cellular trait can be interpreted as the interplay of biochemical properties of molecules and the architecture of gene-regulatory networks (54). Given that regulatory networks are subject to mutation and selection, this implies that the degree of

heterogeneity is an evolvable trait (55). In the context of QS, positive feedback loops (signal auto-regulation (56)) and the presence of cooperative transcription factor binding (57) provides recognized regulatory ingredients for bimodal expression (58). Recently, the presence of heterogeneous QS response at the single-cell scale has been ascribed to a potential bet-hedge against mis-directed QS induction (52), suggesting that our OFF cells are poised to more quickly resume growth in the event of a rapid return to a growth-friendly environment.

We made a number of specific observational choices in order to conduct our experiment that could have shaped our results in ways that are not generalizable to other contexts. In the supplementary we detail a number of additional experiments (and alternate statistical analysis approaches) that collectively illustrate the robustness of our findings. In brief, we found that our single cell results are not sensitive to the time the population was sampled (Figure S5), the presence of a potentially leaky P*lac::lasR* on the pMHLAS construct (Figure S6), or the plasmid nature of the pMHLAS construct (Figure S6). Additionally, we recognize that *lasB* is only one gene out of hundreds that are controlled by QS (3), and is often co-regulated by other factors (59–61). We chose to initially focus on *lasB* as it is a traditionally studied QS-controlled trait (62–64) that has clinical significance as a virulence factor (65, 66). To begin to address the generality of our results across genes in *P. aeruginosa*, we show that two other QS regulated genes with complex promoters, *pqsA* and *rhlI*, also support a graded population response (Figure S7). It remains to be seen whether the graded responses we report here are consistent across all QS controlled genes in *P. aeruginosa*, and across QS systems in other species,

A recent transcriptomic analysis of clinical versus *in vitro* gene expression in *P. aeruginosa* called into question the clinical relevance of *in vitro* models of QS, reporting that QS activity (including *lasB* expression) was systematically higher in *in vitro* models (67). Our results provide a simple interpretation of this difference: *in vitro* models are conducted under higher experimental densities, resulting in higher levels of average QS gene expression (Figure 2). Consistent with this graded response interpretation, Cornforth et al. (2018) also reported higher levels of relative expression in *in vitro* biofilm models (close-packed cells, the highest local density achievable) compared to *in vitro* planktonic models.

In summary, our results provide a finely resolved mapping of the QS reaction norm to environmental density in PAO1, on both the collective and single-cell scale. On the population scale we see a graded linear response across a range of cellular densities ($1x10^8$ cells/ml to $2x10^9$ cells/ml) and significant individual-scale bimodality at higher densities. We further resolve this linear population response (Figure 2) into a combination of the likelihood of being responsive and the intensity of response (Figure 4). The underlying signal dynamics support a threshold

onset of signal auto-induction at intermediate densities, leading to increased levels of QS signal production (Figure 5). In an infection context, our results indicate that there is no hard threshold separating sub-quorate 'stealth' mode and a quorate 'attack' mode (68). One implication is that attempts to control virulence and biofilm expression in medicine and industry via QS inhibition could have impacts across a wider spectrum of population densities. In this applied context, it is important to assess the generality of our results and ask, how do QS reaction-norms vary across strains and species of QS bacteria? How do they vary across environments? More broadly, our work undermines the threshold concept of a 'quorum', instead placing QS bacteria in the graded world of reaction norms.

Materials and Methods

Bacterial Strains and Growth Conditions. The two main bacterial strains used in this study are *P. aeruginosa* NPAO1 (Nottingham-PAO1) containing the *PlasB::gfp(ASV)* quorum sensing reporter pMHLAS (37) and a double signal synthase mutant incapable of producing QS signal molecules, *P. aeruginosa* NPAO1 *ΔlasI/ΔrhlI* containing the same *PlasB::gfp(ASV)* quorum sensing reporter pMHLAS. A complete table of strains used in the main text and supplemental figures can be found in Supplemental Table 1. Overnight cultures were grown in lysogeny broth (LB), supplemented with 50 ug/ml gentamicin to maintain the pMHLAS plasmid, with shaking at 37 °C. Experiments were conducted in lightly buffered (50 mM MOPS) M9 minimal defined media composed of an autoclaved basal salts solution (Na_2HPO_4, 6.8 gL^{-1}; KH_2PO_4, 3.0 gL^{-1}; NaCl, 0.5 gL^{-1}), and filter-sterilized 1 mM $MgSO_4$, 100 uM $CaCl_2$, and 1X Hutner's Trace Elements with casein (CAA) as the sole carbon source.

Controlling Culture Carrying Capacity. We manipulated density by controlling the limiting resource in the media, carbon, allowing us to tune the carrying capacity of each treatment (Figure S1). To cover a variety of densities, we generated a CAA range between 0.05% and 0.25% via dilutions of a 0.5% CAA minimal media stock for a total of 13 different carrying capacities with three replicates each. This produced a range of densities environments from $1.18x10^8$ cells/ml to $2.02x10^9$ cells/ml. Overnight cultures were grown in LB gentamicin 50 ug/ml and centrifuged at 8,500 x g for 2 minutes. The cells were then washed twice with carbonless minimal media and then each carbon treatment was adjusted to OD_{600} = 0.05. Then, 200 uL of each sample was added to a 96-well microplate. Plates were incubated with continuous shaking at 37 °C in a Cytation/BioSpa plate reader and growth curves were generated by absorbance readings taken at 30-min intervals.

Measuring Population QS Response. To measure population response, we performed growth-curve experiments as previously described using PAO1 *PlasB::gfp(ASV)*, additionally taking fluorescence readings at 30-min intervals. Fluorescence, population level response, was recorded when populations reached the end of their exponential growth phase, before they entered stationary phase. Controls for background fluorescence of the reporter were done with the QS signal deficient mutant PAO1 *ΔlasI/ΔrhlI PlasB::gfp(ASV).* The population microplate data (Figure S2) and averaged microscope data (Figure 2) agreed, so the latter is provided in the primary text.

Measuring Individual QS Response. To measure individual response, we performed growth-curve experiments as previously described, but removed samples for microscopy once cells reached end exponential phase. Since we control carrying capacity with the amount of carbon, the exact time that cells reach the end of exponential growth differs across treatments by 2-3 hours. To robustly sample cultures at this specific point, the slope of the two most recent time points on the growth curve was monitored and samples were taken as the slope approached 0. Replicate wells were kept growing to confirm that the treatment entered stationary phase right after the sampling time point. We also determined that our results are generalizable even when sampling at a pre-determined hour across concentrations (Figure S5). Samples were stained with propidium iodide to differentiate between life and dead cells and a small aliquot (5 ul) was added to a 0.01% poly-l-lysine coated slide to immobilize cells and immediately imaged to avoid changes in expression between sample acquisition and imaging in the dark on a Nikon Eclipse TI inverted microscope at 20x magnification. Live cell fluorescence microscopy was used for this study as fluorophores can be sensitive to fixation/permeabilization. These techniques can result in a decrease in fluorescence and therefore decrease in the observable dynamic range. Bright field, green fluorescence (20% Lumencor light engine power, 200ms exposure, and 64x gain-sufficient for imaging of low fluorescent cells without saturating pixel intensity), and red fluorescence (20% Lumencor light engine power, 800ms exposure, and 64x gain) channels were captured. Between 5,000 and 15,000 individual cells were captured for each sample. Aliquots were diluted immediately before imaging with carbonless minimal media when required to ensure an even distribution of cells.

Single cell image analysis. A custom macro in ImageJ was written to analyze the image, outlined in Figure S8. The macro uses ImageJ's "analyze particles" command to identify single cells on the bright field image. This then generates a ROI (region of interest) for each individual cell and these ROIs were then overlaid onto the corresponding fluorescent image. The red fluorescence channel was used to identify dead cells with compromised membranes, which were excluded from further analysis. The green fluorescence channel reflected the QS reporter and pixel intensity was measured as a proxy for level of QS response. This tabulated live cell

expression data was then analyzed using *Stata Statistical Software: Release 17* from StataCorp LLC. In order to improve the fit of the mixed models, the lowest pixel intensity measurement in the highest carbon PAO1 *ΔlasI/ΔrhlI PlasB::gfp(ASV)* treatment was subtracted from all pixel intensities so that expression started at 0.

Statistical analysis summary. The analysis was done using *Stata Statistical Software: Release 17* from StataCorp LLC and the additional third party resources: (69–73). Each of the 39 populations was fit to a finite mixture model of two Gamma distributions. The latent classes in the mixture model correspond to OFF and ON cells. Gamma distributions are preferred to Normal distributions as gene expression is strictly non-negative and necessarily right-skewed. The models provide maximum likelihood estimates of the proportion of cells in each latent class and the shape and scale parameters of the component Gamma distributions. Mean expression level for each distribution is the product of shape and scale parameters. Information criteria for aggregate mean expression level was also calculated using Stata.

Quantifying Signal Concentration. AHL signal concentration was estimated using S17-1 *Escherichia coli* containing either the p56536 or pSB1142 plasmids (74), which luminesce in response to short and long chain AHLs, respectively. Filtered culture supernatant was diluted 1/100 in LB broth and mixed 1:1 with exponentially growing bioreporter strains at an OD_{600} of 0.1 in LB broth. A calibration curve was generated by exposing the bioreporters to synthetic signal at various concentrations. Signal bioreporters were grown with diluted supernatant for 3 hours at 37 °C taking reads of optical density and luminescence every 30 min. Using the peak luminesce, a calibration curve was then fitted to calculate signal concentrations in experimental samples.

Acknowledgments

We thank Steve Diggle, Marvin Whitely, Kathleen O'Connor and members of the Center for Microbial Dynamics and Infection (CMDI) for valuable comments and discussion on this work. We thank Dr. Kasper Norskov Kragh for the *PlasB::gfp(ASV)* reporter construct. This research was supported by the National Science Foundation Graduate Research Fellowship Program under Grant No. DGE-1650044 and by The Simons Foundation Grant No. 396001.

References

1. S. T. Rutherford, B. L. Bassler, Bacterial quorum sensing: Its role in virulence and possibilities for its control. *Cold Spring Harb. Perspect. Med.* **2** (2012).

2. R. G. Abisado, S. Benomar, J. R. Klaus, A. A. Dandekar, J. R. Chandler, Bacterial Quorum Sensing and Microbial Community Interactions. *MBio* **9**, e02331-17 (2018).

3. M. Whiteley, S. P. Diggle, E. P. Greenberg, Progress in and promise of bacterial quorum sensing research. *Nature* **551**, 313–320 (2017).

4. M. B. Miller, B. L. Bassler, Quorum Sensing in Bacteria. *Annu. Rev. Microbiol.* **55**, 165–199 (2001).

5. R. Popat, D. M. Cornforth, L. McNally, S. P. Brown, Collective sensing and collective responses in quorum-sensing bacteria. *J. R. Soc. Interface* **12** (2015).

6. S. E. Darch, S. A. West, K. Winzer, S. P. Diggle, Density-dependent fitness benefits in quorum-sensing bacterial populations. *Proc. Natl. Acad. Sci.* **109**, 8259–8263 (2012).

7. R. J. Redfield, Is quorum sensing a side effect of diffusion sensing? *Trends Microbiol.* **10**, 365–70 (2002).

8. B. A. Hense, *et al.*, Does efficiency sensing unify diffusion and quorum sensing? *Nat. Rev. Microbiol.* **5**, 230–239 (2007).

9. J. Q. Boedicker, M. E. Vincent, R. F. Ismagilov, Microfluidic Confinement of Single Cells of Bacteria in Small Volumes Initiates High-Density Behavior of Quorum Sensing and Growth and Reveals Its Variability. *Angew. Chemie Int. Ed.* **48**, 5908–5911 (2009).

10. D. M. Cornforth, *et al.*, Combinatorial quorum sensing allows bacteria to resolve their social and physical environment. *Proc. Natl. Acad. Sci. U. S. A.* **111**, 4280–4284 (2014).

11. R. C. Allen, L. McNally, R. Popat, S. P. Brown, Quorum sensing protects bacterial co-operation from exploitation by cheats. *ISME J.* **10**, 1706–1716 (2016).

12. A. Eldar, Social conflict drives the evolutionary divergence of quorum sensing. *Proc. Natl. Acad. Sci. U. S. A.* **108**, 13635–13640 (2011).

13. N. E. Smalley, D. An, M. R. Parsek, J. R. Chandler, A. A. Dandekar, Quorum Sensing Protects Pseudomonas aeruginosa against Cheating by Other Species in a Laboratory Coculture Model. *J. Bacteriol.* **197**, 3154 LP – 3159 (2015).

14. E. Even-Tov, *et al.*, Social Evolution Selects for Redundancy in Bacterial Quorum Sensing. *PLOS Biol.* **14**, e1002386 (2016).

15. E. T. Granato, R. Kümmerli, The path to re-evolve cooperation is constrained in Pseudomonas aeruginosa. *BMC Evol. Biol.* **17**, 214 (2017).

16. Ö. Özkaya, R. Balbontín, I. Gordo, K. B. Xavier, Cheating on Cheaters Stabilizes Cooperation in Pseudomonas aeruginosa. *Curr. Biol.* **28**, 2070-2080.e6 (2018).

17. R. Chen, E. Déziel, M. C. Groleau, A. L. Schaefer, E. P. Greenberg, Social cheating in a Pseudomonas aeruginosa quorum-sensing variant. *Proc. Natl. Acad. Sci. U. S. A.* **116**, 7021–7026 (2019).

18. J. Gurney, S. Azimi, S. P. Brown, S. P. Diggle, Combinatorial quorum sensing in Pseudomonas aeruginosa allows for novel cheating strategies. *Microbiology*, micro000941 (2020).

19. J. L. Connell, *et al.*, Probing prokaryotic social behaviors with bacterial “lobster traps.” *MBio* **1** (2010).

20. W. C. Fuqua, S. C. Winans, E. P. Greenberg, Quorum sensing in bacteria: The LuxR-LuxI family of cell density- responsive transcriptional regulators. *J. Bacteriol.* **176**, 269–275 (1994).

21. J. Schluter, A. P. Schoech, K. R. Foster, S. Mitri, The Evolution of Quorum Sensing as a Mechanism to Infer Kinship. *PLOS Comput. Biol.* **12**, e1004848 (2016).

22. Y. Wang, J. B. Rattray, S. A. Thomas, J. Gurney, S. P. Brown, In silico bacteria evolve robust cooperaion via complex quorum-sensing strategies. *Sci. Rep.* **10**, 1–10 (2020).

23. A. B. Goryachev, Understanding Bacterial Cell−Cell Communication with Computational Modeling. *Chem. Rev.* **111**, 238–250 (2011).

24. S. James, P. Nilsson, G. James, S. Kjelleberg, T. Fagerström, Luminescence control in the marine bacterium Vibrio fischeri: An analysis of the dynamics of lux regulation. *J. Mol. Biol.* **296**, 1127–1137 (2000).

25. Woltereck, Weitere experimentelle Untersuchungen uber Artveranderung, speziel uber das Wesen quantitativer Artuntershiede bei Daphniden. *Science (80-.).* **32**, 344–345 (1910).

26. C. H. Waddington, Canalization of development and the inheritance of acquired characters. *Nature* **150**, 563–565 (1942).

27. C. Schlichting, M. Pigliucci, Phenotypic Evolution: A Reaction Norm Perspective (1998).

28. A. B. Paaby, N. D. Testa, "Developmental Plasticity and Evolution" in *Evolutionary Developmental Biology*, (Springer International Publishing, 2018), pp. 1–14.

29. R. L. Scholz, E. Peter Greenberg, Positive autoregulation of an Acyl- homoserine lactone quorum-sensing circuit synchronizes the population response. *MBio* **8** (2017).

30. B. B. Pradhan, S. Chatterjee, Reversible non-genetic phenotypic heterogeneity in bacterial quorum sensing. *Mol. Microbiol.* **92**, 557–569 (2014).

31. C. Anetzberger, T. Pirch, K. Jung, Heterogeneity in quorum sensing-regulated bioluminescence of *Vibrio harveyi*. *Mol. Microbiol.* **73**, 267–277 (2009).

32. P. D. Pérez, S. J. Hagen, Heterogeneous response to a quorum-sensing signal in the luminescence of individual vibrio fischeri. *PLoS One* **5** (2010).

33. J. Grote, D. Krysciak, W. R. Streit, Phenotypic heterogeneity, a phenomenon that may explain why quorum sensing does not always result in truly homogenous cell behavior. *Appl. Environ. Microbiol.* **81**, 5280–5289 (2015).

34. D. Garmyn, *et al.*, Evidence of autoinduction heterogeneity via expression of the agr system of Listeria monocytogenes at the single-cell level. *Appl. Environ. Microbiol.* **77**, 6286–6289 (2011).

35. E. L. Haseltine, F. H. Arnold, Implications of rewiring bacterial quorum sensing. *Appl. Environ. Microbiol.* **74**, 437–445 (2008).

36. L. Plener, *et al.*, The Phosphorylation Flow of the Vibrio harveyi Quorum-Sensing Cascade Determines Levels of Phenotypic Heterogeneity in the Population. *J. Bacteriol.* **197**, 1747 (2015).

37. M. Hentzer, *et al.*, Inhibition of quorum sensing in Pseudomonas aeruginosa biofilm bacteria by a halogenated furanone compound. *Microbiology* **148**, 87–102 (2002).

38. K. P. Burnham, D. R. Anderson, K. P. Huyvaert, AIC model selection and multimodel inference in behavioral ecology: some background, observations, and comparisons. *Behav. Ecol. Sociobiol. 2010 651* **65**, 23–35 (2010).

506 39. J. A. Hartigan, P. M. Hartigan, The Dip Test of Unimodality.
507 *https://doi.org/10.1214/aos/1176346577* **13**, 70–84 (1985).

508 40. S. PC, P. L, I. BH, Activation of the Pseudomonas aeruginosa lasI gene by LasR and the
509 Pseudomonas autoinducer PAI: an autoinduction regulatory hierarchy. *J. Bacteriol.* **177**,
510 654–659 (1995).

511 41. M. LM, W. M, Membrane vesicles traffic signals and facilitate group activities in a
512 prokaryote. *Nature* **437**, 422–425 (2005).

513 42. K. Papenfort, B. L. Bassler, Quorum sensing signal–response systems in Gram-negative
514 bacteria. *Nat. Rev. Microbiol. 2016 149* **14**, 576–588 (2016).

515 43. L. J, Z. L, The hierarchy quorum sensing network in Pseudomonas aeruginosa. *Protein*
516 *Cell* **6**, 26–41 (2015).

517 44. D. V, D. E, Revisiting the quorum-sensing hierarchy in Pseudomonas aeruginosa: the
518 transcriptional regulator RhlR regulates LasR-specific factors. *Microbiology* **155**, 712–723
519 (2009).

520 45. J. B. Feltner, *et al.*, LasR variant cystic fibrosis isolates reveal an adaptable quorum-
521 sensing hierarchy in Pseudomonas aeruginosa. *MBio* **7** (2016).

522 46. S.-A. MP, *et al.*, Inactivation of the quorum-sensing transcriptional regulators LasR or
523 RhlR does not suppress the expression of virulence factors and the virulence of
524 Pseudomonas aeruginosa PAO1. *Microbiology* **165**, 425–432 (2019).

525 47. C. RL, *et al.*, RhlR-Regulated Acyl-Homoserine Lactone Quorum Sensing in a Cystic
526 Fibrosis Isolate of Pseudomonas aeruginosa. *MBio* **11** (2020).

527 48. W. MK, *et al.*, Construction and analysis of luxCDABE-based plasmid sensors for
528 investigating N-acyl homoserine lactone-mediated quorum sensing. *FEMS Microbiol. Lett.*
529 **163**, 185–192 (1998).

530 49. , The evolutionary consequences of plasticity in host–pathogen interactions -
531 ScienceDirect (November 10, 2019).

532 50. S. Via, *et al.*, Adaptive phenotypic plasticity: consensus and controversy. *Trends Ecol.*
533 *Evol.* **10**, 212–217 (1995).

534 51. S. Heilmann, S. Krishna, B. Kerr, Why do bacteria regulate public goods by quorum
535 sensing?-How the shapes of cost and benefit functions determine the form of optimal
536 regulation. *Front. Microbiol.* **6** (2015).

537 52. P. Jayakumar, S. A. Thomas, S. P. Brown, R. Kümmerli, Pseudomonas aeruginosa
538 reaches collective decisions via transient segregation of quorum sensing activities across
539 cells. *bioRxiv*, 2021.03.22.436499 (2021).

540 53. S. E. Darch, *et al.*, Spatial determinants of quorum signaling in a Pseudomonas
541 aeruginosa infection model. *Proc. Natl. Acad. Sci.* **115**, 4779–4784 (2018).

542 54. K. Fujimoto, S. Sawai, A Design Principle of Group-level Decision Making in Cell
543 Populations. *PLOS Comput. Biol.* **9**, e1003110 (2013).

544 55. M. Ackermann, A functional perspective on phenotypic heterogeneity in microorganisms.
545 *Nat. Rev. Microbiol. 2015 138* **13**, 497–508 (2015).

546 56. J. L. Cherry, F. R. Adler, How to make a Biological Switch. *J. Theor. Biol.* **203**, 117–133

(2000).

57. M. Schuster, M. L. Urbanowski, E. P. Greenberg, Promoter specificity in Pseudomonas aeruginosa quorum sensing revealed by DNA binding of purified LasR. *Proc. Natl. Acad. Sci.* **101**, 15833–15839 (2004).

58. A. Ochab-Marcinek, M. Tabaka, Bimodal gene expression in noncooperative regulatory systems. *Proc. Natl. Acad. Sci.* **107**, 22096–22101 (2010).

59. B. Mellbye, M. Schuster, Physiological framework for the regulation of quorum sensing-dependent public goods in Pseudomonas aeruginosa. *J. Bacteriol.* **196**, 1155–1164 (2014).

60. S. P. Diggle, K. Winzer, A. Lazdunski, P. Williams, M. Cámara, Advancing the quorum in Pseudomonas aeruginosa: MvaT and the regulation of N-acylhomoserine lactone production and virulence gene expression. *J. Bacteriol.* **184**, 2576–2586 (2002).

61. S. A. Chugani, *et al.*, QscR, a modulator of quorum-sensing signal synthesis and virulence in Pseudomonas aeruginosa. *Proc. Natl. Acad. Sci. U. S. A.* **98**, 2752–2757 (2001).

62. M. J. Gambello, B. H. Iglewski, Cloning and characterization of the Pseudomonas aeruginosa lasR gene, a transcriptional activator of elastase expression. *J. Bacteriol.* **173**, 3000 (1991).

63. J. P. Pearson, L. Passador, B. H. Iglewski, E. P. Greenberg, A second N-acylhomoserine lactone signal produced by Pseudomonas aeruginosa. *Proc. Natl. Acad. Sci.* **92**, 1490–1494 (1995).

64. B. JM, O. DE, Synthesis of multiple exoproducts in Pseudomonas aeruginosa is under the control of RhlR-RhlI, another set of regulators in strain PAO1 with homology to the autoinducer-responsive LuxR-LuxI family. *J. Bacteriol.* **177**, 7155–7163 (1995).

65. C. F, *et al.*, The LasB Elastase of Pseudomonas aeruginosa Acts in Concert with Alkaline Protease AprA To Prevent Flagellin-Mediated Immune Recognition. *Infect. Immun.* **84**, 162–171 (2015).

66. C. Cigana, *et al.*, Pseudomonas aeruginosa Elastase Contributes to the Establishment of Chronic Lung Colonization and Modulates the Immune Response in a Murine Model. *Front. Microbiol.* **0**, 3443 (2021).

67. D. M. Cornforth, *et al.*, Pseudomonas aeruginosa transcriptome during human infection. *Proc. Natl. Acad. Sci.* **115**, E5125–E5134 (2018).

68. K. Winzer, P. Williams, Quorum sensing and the regulation of virulence gene expression in pathogenic bacteria. *Int. J. Med. Microbiol.* **291**, 131–143 (2001).

69. N. J. Cox, DIPTEST: Stata module to compute dip statistic to test for unimodality. *Stat. Softw. Components* (2016) (November 8, 2021).

70. N. J. Cox, S. P. Jenkins, GAMMAFIT: Stata module to fit a two-parameter gamma distribution. *Stat. Softw. Components* (2011) (November 8, 2021).

71. P. Deb, FMM: Stata module to estimate finite mixture models. *Stat. Softw. Components* (2012) (November 8, 2021).

72. B. Jann, PALETTES: Stata module to provide color palettes, symbol palettes, and line pattern palettes. *Stat. Softw. Components* (2020) (November 8, 2021).

588 73. B. Jann, COLRSPACE: Stata module providing a class-based color management system
589 in Mata. *Stat. Softw. Components* (2020) (November 8, 2021).

590 74. M. K. Winson, *et al.*, Construction and analysis of luxCDABE -based plasmid sensors for
591 investigating N -acyl homoserine lactone-mediated quorum sensing . *FEMS Microbiol.*
592 *Lett.* **163**, 185–192 (1998).

593 75. J. Meisner, J. B. Goldberg, The Escherichia coli rhaSR-PrhaBAD inducible promoter
594 system allows tightly controlled gene expression over a wide range in Pseudomonas
595 aeruginosa. *Appl. Environ. Microbiol.* **82**, 6715–6727 (2016).

596 76. F. MP, *et al.*, A dual biosensor for 2-alkyl-4-quinolone quorum-sensing signal molecules.
597 *Environ. Microbiol.* **9**, 2683–2693 (2007).

598 77. H. TT, K. AJ, B. A, S. HP, Integration-proficient plasmids for Pseudomonas aeruginosa:
599 site-specific integration and use for engineering of reporter and expression strains.
600 *Plasmid* **43**, 59–72 (2000).

601 78. N. Friedman, L. Cai, X. S. Xie, Linking Stochastic Dynamics to Population Distribution: An
602 Analytical Framework of Gene Expression. *Phys. Rev. Lett.* **97**, 168302 (2006).

603 79. A. P. Dempster, N. M. Laird, D. B. Rubin, Maximum Likelihood from Incomplete Data via
604 the EM Algorithm. *J. R. Stat. Soc. Ser. B* **39**, 1–38 (1977).

605 80. T. L. Bailey, C. Elkan, Fitting a mixture model by expectation maximization to discover
606 motifs in biopolymers. *Proceedings. Int. Conf. Intell. Syst. Mol. Biol.* **2**, 28–36 (1994).

607 81. J. Abrevaya, W. Jiang, A Nonparametric Approach to Measuring and Testing Curvature. *J.*
608 *Bus. Econ. Stat.* **23**, 1–19 (2005).

609 82. G. C. Chow, Tests of Equality Between Sets of Coefficients in Two Linear Regressions.
610 *Econometrica* **28**, 591–605 (1960).

611